symmetry

MDPI

Article

Dense Cold Quark–Gluon Matter Clusters and Their Study at the NICA Collider

Vladimir Vechernin *, Svetlana Belokurova and Semyon Yurchenko

Laboratory of Ultra-High Energy Physics, Saint-Petersburg State University, 7-9 Universitetskaya emb., 199034 St. Petersburg, Russia; sveta.1596@mail.ru (S.B.); semyon.yurchenko@luhep.ru (S.Y.)
* Correspondence: v.vechernin@spbu.ru

Abstract: In this paper, the production of particles outside the region of nucleon–nucleon kinematics due to interactions involving dense cold clusters of quark-gluon matter in nuclei is calculated. The possibility of observing this process in the region of central rapidities and large transverse momenta in heavy ion collisions at low energies with MPD detector at the NICA collider is demonstrated.

Keywords: strong interaction; high energy; dense cold nuclear matter; quark–gluon clusters; multinucleon fluctons; cumulative particle production; central rapidities; large transverse momentum; NICA collider

PACS: 12.39.Mk; 13.60.Hb; 21.60.Gx

check for updates

Citation: Vechernin, V.; Belokurova, S.; Yurchenko, S. Dense Cold Quark–Gluon Matter Clusters and Their Study at the NICA Collider. *Symmetry* **2024**, *16*, 79. https://doi.org/10.3390/sym16010079

Academic Editor: Jorge Segovia

Received: 2 December 2023
Revised: 28 December 2023
Accepted: 29 December 2023
Published: 6 January 2024

1. Introduction

Long ago, in experiments [1,2] on the interaction of high-energy protons with nuclei, an unexpectedly large yield of particles into the rear hemisphere was discovered in a region where nucleon–nucleon interaction is kinematically forbidden. This served as the basis for putting forward a hypothesis [3] about the presence of nuclear density fluctuations in nuclei, called “fluctons”. It was assumed that, in a target nucleus, two or even more nucleons can periodically approach each other at short distances, forming a cluster of several nucleons. In this case, the interaction of an incident proton with such a multinucleon cluster (flucton) makes it possible to explain the observed particle production in the backward direction, outside the region permitted by nucleon–nucleon kinematics. Later, this area of momenta was referred to as cumulative.

In time, when the first beams of relativistic nuclei were obtained, it became possible to study cumulative production in the region of projectile nucleus fragmentation [4,5]. In this case, it corresponds to the production of particles with a longitudinal momentum greater than that the per-nucleon momentum of the incident nuclei, which explains the name of “cumulative production”. In both cases, experimental studies of this phenomenon in the regions of fragmentation of the target nucleus and the projectile nucleus are limited to the region of rather small transverse momenta (less than 2 GeV) [6–10].

A variety of models has been suggested to describe the process of of particle formation in the cumulative region. These can be conditionally divided into two large groups. The first group [11–21] assumes the presence of fluctons in the initial state of the nucleus, while the second [22–25] suggests that the dense nuclear matter clusters are formed later, in the process of a nuclear collision.

Currently, the construction of the NICA collider at JINR in Dubna [26–29], designed for relatively low energies of colliding nuclei compared to the LHC and RHIC colliders as well as high luminosity, has opened up the possibility of studying the production of particles in a new cumulative region of central rapidities and large transverse momenta. These investigations are of great interest, as from the contemporary point of view multinucleon fluctons in nuclei are clumps of dense cold baryon-enriched quark–gluon matter. Studies of the clusters of dense cold quark–gluon matter intrinsic to the nuclei (see [30]) are expected to be possible in future experiments at FAIR (Darmstadt).

In the present paper, we study the possibility of observing particle production in the new cumulative region of central rapidities and large transverse momenta in Au–Au collisions using the MPD installation at the NICA complex. We estimate the yield of pions and protons in this new cumulative region caused by the process in which a nucleon of one nucleus interacts with a flucton from another. To describe the dependence of cumulative particles on transverse momentum, we use a microscopic (at the quark level) approach developed earlier [16–21] to describe the cumulative particle production in the fragmentation region of one of these colliding nuclei.

2. Features of Cumulative Production in the Nucleus Fragmentation Region

Most of the experimental data on cumulative production were obtained in the rest frame of a fragmenting nucleus. In this case, when incident protons are scattered on a fixed target nucleus, cumulative particles are emitted into the rear hemisphere, which is convenient for the experimental study of this process.

For the inclusive cross-section of particle production in the cumulative region in pA collisions,

$$\mathrm{p} + \mathrm{A} \to \mathrm{c} + \mathrm{X},$$

and the so-called nuclear scaling was experimentally established as follows:

$$\frac{k_0\, d^3\sigma}{A\, d^3\mathbf{k}} = f(x, k_\perp)\,. \tag{1}$$

As a scaling variable x, it was proposed to use the so-called cumulative number x, defined as the minimum target mass (measured in nucleon masses), that allows the production of a cumulative particle c with a given momentum k. This variable is suitable because for an integer $x = 1, 2, 3, \ldots$ it determines the kinematic boundaries for the production of a particle c with momentum k when an incident proton collides with a flucton consisting of x nucleons (see Figures 1 and 2).

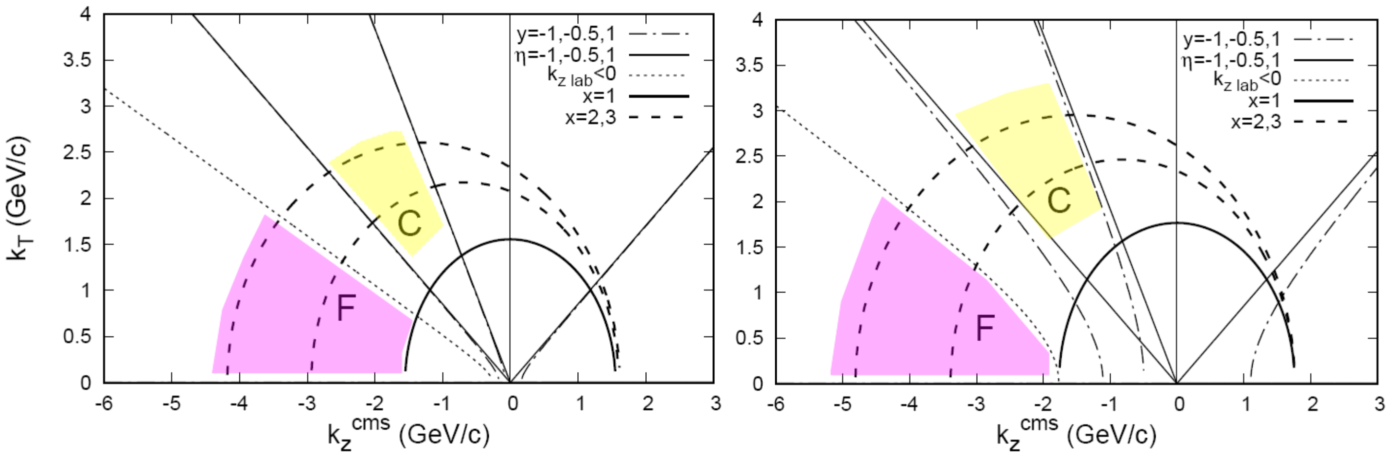

Figure 1. Kinematic boundaries for the production of pions (**left** panel) and protons (**right** panel) in the collision of a proton with a cluster consisting of x nucleons (thick dashed curve) at the initial energy $\sqrt{s_{NN}}$ = 4 GeV in the center-of-mass system of NN collision. The thick solid curve ($x = 1$) is the boundary of the cumulative region (production outside the NN kinematics). The dash-dotted curves and thin solid thin lines present the rapidity ($-1 < y < 1$) and pseudorapidity ($-1 < \eta < 1$) acceptance of the NICA MPD. The dotted curve is the boundary of the region F, which corresponds to the production in the rear hemisphere in the rest frame of a fragmenting nucleus ($k_z^{lab} < 0$).

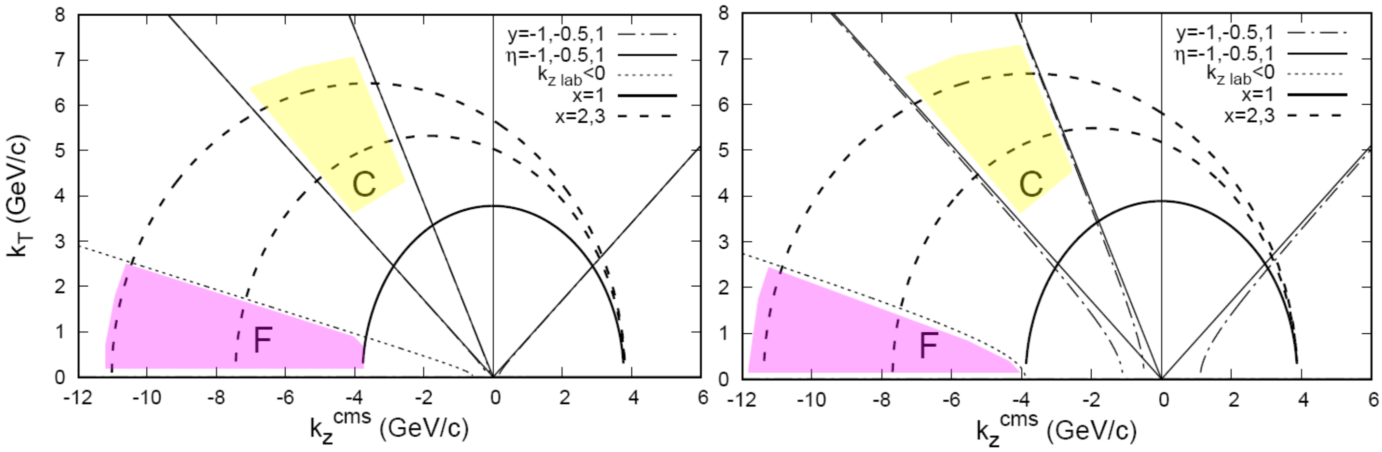

Figure 2. The same as in Figure 1, except for an initial energy $\sqrt{s_{NN}}$ = 8 GeV.

The variable x is relativistically invariant, and can be calculated in an arbitrary frame of reference from the equation

$$(k, p_1) + x(k, p_2) = \bar{s}(x)/2\,. \tag{2}$$

Here, p_1 is the 4-momentum of the incident proton and p_2 is the 4-momentum per nucleon in nucleus A. The $\bar{s}(x)$ is equal to

$$\bar{s}_\pi(x) = x(s - 4m^2) + \mu^2 \tag{3}$$

for production of pions and

$$\bar{s}_p(x) = x(s - 2m^2) + 2m^2 \tag{4}$$

for production of protons. Here, μ is the mass of the produced particle c, m is the nucleon mass, and $s = (p_1 + p_2)^2 \equiv s_{NN}$ (for more details, see [31]).

For pA interaction at relativistic energies, as follows from the data (see for example the analysis in the articles [6,8–10]), the function $f(x, k_\perp)$ in (1) does not depend on either the initial energy ($\sqrt{s} = \sqrt{s_{NN}}$) or the atomic number of the nucleus A (at least for heavy nuclei). It can be presented in the following form:

$$f(x, k_\perp) = C_0\, e^{-x/x_0}\, \phi(x, k_\perp)\,, \tag{5}$$

where

$$\phi(x, k_\perp) \equiv f(x, k_\perp)/f(x, 0)\,, \qquad \phi(x, 0) = 1\,. \tag{6}$$

The value of the parameter x_0 in (5) is 0.139 for pions and 0.135 for protons, and the exponential dependence is well satisfied at $x > 1.2$ for pions and $x > 1.6$ for protons [10]. Please note that for the production of pions and protons, $C_{0\pi} = 4.0 \cdot 10^2$ and $C_{0p} = 2.64 \cdot 10^6$ mb/Gev^2; thus, the yield of cumulative protons in the region of nuclear fragmentation (region F in Figures 1 and 2) is almost 10^4 times higher compared to that of pions.

As for the dependence of the yields of cumulative particles on the transverse momentum, in [9,10], when analyzing experimental data, it was parameterized by the Gaussian dependence:

$$\phi(x, k_\perp) = e^{-k_\perp^2/\langle k_\perp^2\rangle} \tag{7}$$

the parameter $\langle k_\perp^2 \rangle$ increases with the cumulative number x and depends on the kind of particle under investigation. These dependencies can be parameterized for pion and proton production as follows [31]:

$$\langle k_\perp^2 \rangle_\pi(x) = 0.3 + 0.8(x - 1.2) \qquad \langle k_\perp^2 \rangle_{\rm p}(x) = 0.19 + 0.42(x - 1.6) \tag{8}$$

where the square of the transverse momentum is measured in $\mathrm{GeV}^2/\mathrm{c}^2$.

This Gaussian approximation (7), used in [9,10], does not seem quite realistic to us, especially in light of the extrapolation of this dependence to the region of sufficiently large transverse momenta (region C in Figures 1 and 2). Therefore, in the works [31,32] we proposed an alternative parameterization of the dependence of the data [9,10] on the transverse momentum by a simple exponent, which usually provides a more adequate description of the data for large transverse momenta:

$$\phi(x, k_\perp) = e^{-2k_\perp/\bar{k}_\perp}\,, \tag{9}$$

where

$$\bar{k}^2_{\perp\pi}(x) = 0.6 + 1.4(x - 1.2)\,, \qquad \bar{k}^2_{\perp{\rm p}}(x) = 0.14 + 0.32(x - 1.6)\,. \tag{10}$$

Unfortunately, as shown in [31,32], although both approximations provide an adequate description of the experimental data [9,10] in the nucleus fragmentation region (region F in Figures 1 and 2), they provide very different results, especially at higher initial energy ($\sqrt{s_{NN}}$ = 8 GeV), when we use them to calculate particle yields in the new cumulative region of central rapidities and large transverse momenta (region C in Figures 1 and 2) available for study at the NICA MPD. In these figures, we depict the pseudorapidity acceptance ($-1 < \eta < 1$) of the MPD detector in the NN collision center of the mass frame. Region F corresponds to the production in the rear hemisphere in the rest frame of a fragmenting nucleus ($k_z^{lab} < 0$).

Comparing Figures 1 and 2, it is apparent that in the new cumulative region the transverse momenta of particles increase with the initial energy. This explains why the study of particle production in this region is absolutely impossible at the LHC and RHIC energies.

3. Theoretical Description of the Dependence on Transverse Momentum in the Cumulative Region

In the present paper, in order to eliminate the uncertainty described at the end of the previous section and estimate the yield of pions and protons with large transverse momenta in the new cumulative region of mid-rapidities at NICA energies, we use the quark–parton model of the cumulative particle production from a flucton, which was developed earlier [16–21].

As shown in this model, the formation of cumulative pions and protons is dominated by two different mechanisms. In the case of pion production, the fragmentation of one flucton quark into a pion predominates [16–18] (see the left panel in Figure 3), whereas in the case of proton production, the mechanism of coherent coalescence (recombination) of three flucton quarks into a proton is dominant [19–21] (the right panel in Figure 3).

As shown in [21], in the framework of this approach the dependence on transverse momentum for the production of cumulative pions is provided by the expression

$$\phi(x, k_\perp) = \Phi_p\!\left(\frac{k_\perp}{m_q}\right) / \Phi_p(0) \tag{11}$$

where $p = [3x]$ is the number of donor quarks transferring their momentum to the active quark forming a cumulative pion ($[\ldots]$ denotes the integer part) and

$$\Phi_p(t) = 2\pi \int_0^\infty dz\, z\, J_0(tz)[zK_1(z)]^p\,. \tag{12}$$

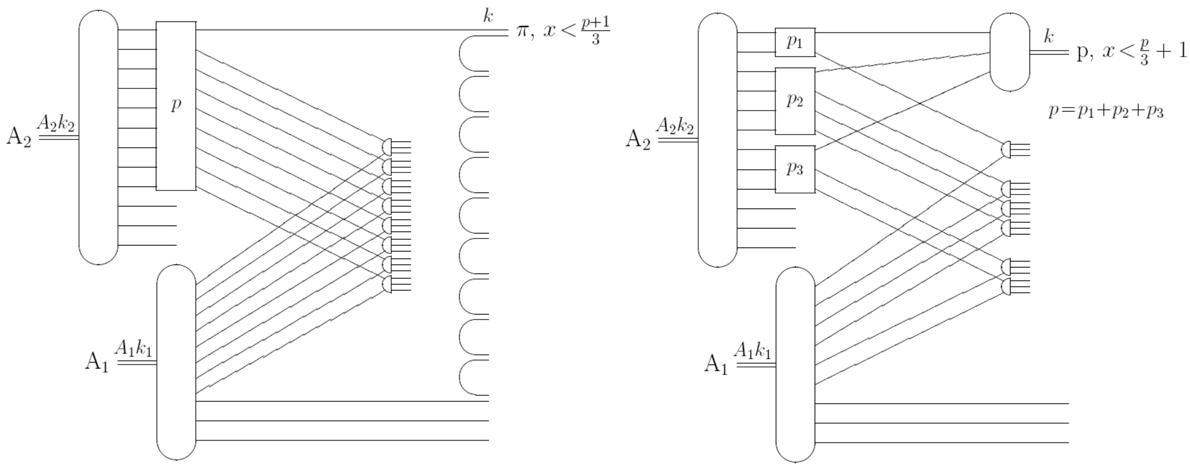

Figure 3. Formation of cumulative pions due to the fragmentation of a single flucton quark into a pion [16–18] (**left** panel) and formation of cumulative protons due to the coherent coalescence (recombination) of three flucton quarks into a proton [19–21] (**right** panel).

Here, $J_0(z)$ is the Bessel function and $K_1(z)$ is the modified Bessel function (McDonald function). Note that for $p = 1$, the integral (12) is calculated explicitly:

$$\Phi_1(t) = \frac{4\pi}{(t^2+1)^2}. \tag{13}$$

The dependence on transverse momentum for the production of cumulative protons is provided by the expression

$$\phi(x, k_\perp) = \Phi_{p_1}\left(\frac{k_\perp}{3m_q}\right)\Phi_{p_2}\left(\frac{k_\perp}{3m_q}\right)\Phi_{p_3}\left(\frac{k_\perp}{3m_q}\right) / \{\Phi_{p_1}(0)\Phi_{p_2}(0)\Phi_{p_3}(0)\}\ , \tag{14}$$

where, for the considered interval of x for protons ($1.6 < x < 4$),

$$p_1 = 1 + \vartheta(x - 8/3) + \vartheta(x - 11/3)\ , \tag{15}$$

$$p_2 = 1 + \vartheta(x - 7/3) + \vartheta(x - 10/3)\ , \tag{16}$$

$$p_3 = 1 + \vartheta(x - 2) + \vartheta(x - 3)\ . \tag{17}$$

where $\vartheta(x)$ is a step function. The total number of donor quarks transferring their momentum to three active quarks forming a cumulative proton is equal to $p = p_1 + p_2 + p_3$.

Note that m_q, which is the constituent quark mass, is the only parameter in these formulas (see (11) and (14)). With a natural value of this parameter, m_q = 310 MeV, we obtain a simultaneous description of the dependence of the production of cumulative pions and protons on the transverse momentum (see Figure 4).

Really, in Figure 4 we see that, with the natural value of a single parameter m_q, this approach correctly describes the broadening of transverse momentum distributions with increasing cumulative number, which is observed for both pion and proton yields. Moreover, at the same time, it provides correct wider transverse momentum distributions for pions compared to protons for the same value of the cumulative variable. In this approach, it arises due to different mechanisms of the formation of particles with momenta outside the pp-kinematics, that is fragmentation of one flucton quark for a pion (left panel in Figure 3) and coherent coalescence (recombination) of three flucton-quarks for a proton (right panel in Figure 3).

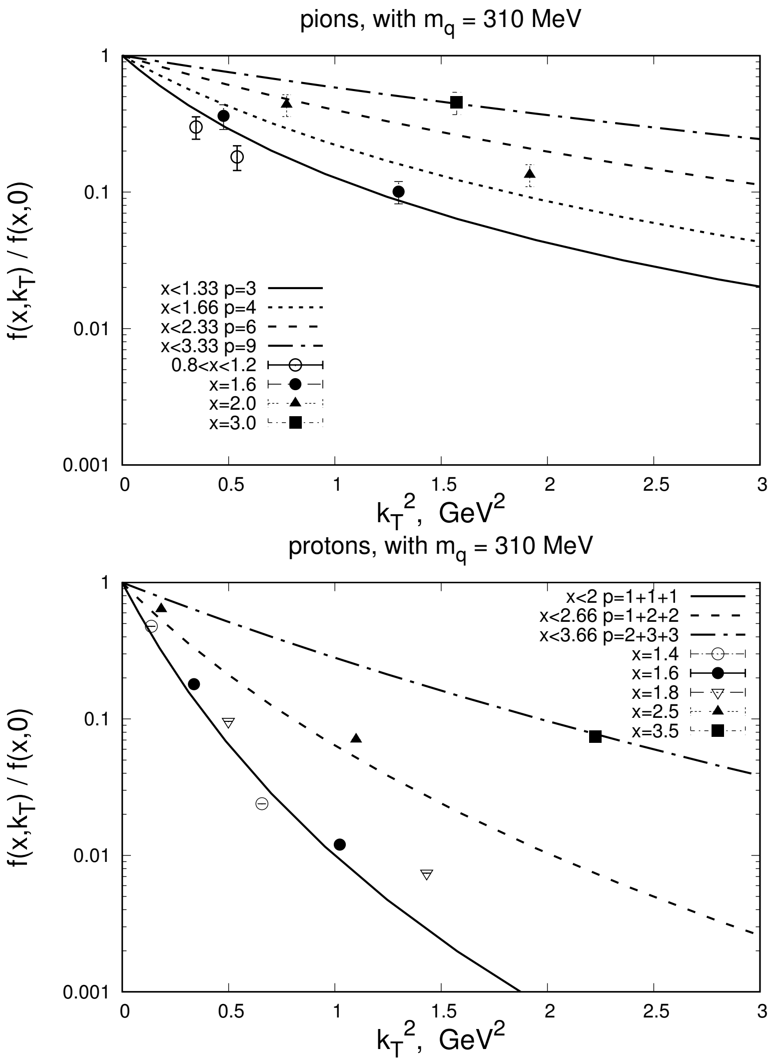

Figure 4. Dependence of the production of cumulative pions (**upper** panel) and protons (**lower** panel) on the transverse momentum $\phi(x, k_\perp) \equiv f(x, k_\perp)/f(x, 0)$ (12), calculated by Formulas (11) and (14) with the value of the only parameter, m_q (the mass of the constituent quark) equal to 310 MeV. For a given value of the cumulative variable x, the number of donor quarks p is calculated as $p = [3x]$ for pion production and as $p = p_1 + p_2 + p_3$ (15) for proton production (see text for details). The corresponding experimental points are taken from the article [9,10].

4. Yield of Cumulative Particles at mid-Rapidities in pA Colllisions

In this section, we estimate the yield of cumulative pions and protons with high transverse momentum at central rapidities in pA collisions using the theoretical description of the dependence of cumulative production on transverse momentum obtained in the previous section. The idea is to use the description of the inclusive cross-section of the cumulative particle production $f(x, k_\perp)$ (1) obtained in the nucleus fragmentation region (region F in Figures 1 and 2), to estimate particle yields in the new cumulative region of central rapidities (region C in Figures 1 and 2), available for study at the NICA collider.

For region C (see Figures 1 and 2), the rapidity interval $-1 < y < -0.5$ is selected. This means that in the center of mass frame, the incident proton moves along the z axis and the fragmenting nucleus moves in the opposite direction. We exclude the region near zero rapidity, as the theoretical approach [16–21] (Figure 3), used in the previous section to describe the transverse momentum dependence of cumulative production is not valid at small k_z^{cms} values.

Comparing the Figures 1 and 2, we expect the results obtained for the initial energy $\sqrt{s_{NN}}$ = 4 GeV to be more reliable than those for $\sqrt{s_{NN}}$ = 8 GeV, as in the latter case it is necessary to extrapolate the cross-section $f(x,k_\perp)$ to significantly higher values of transverse momenta.

Taking into account the definition of $f(x,k_\perp)$ (1), the multiplicity of particles in acceptance Ω in a pA collision is determined by the expression

$$\langle n\rangle^{\Omega}_{\text{pA}} \cdot \sigma^{tot}_{\text{pA}} = A \int_{\Omega} \frac{d^3\mathbf{k}}{k_0}\, f(x,k_\perp). \tag{18}$$

Using the relativistic invariance of $f(x,k_\perp)$ we can write (18) in the center-of-mass system of NN collision and move from k^*_z to rapidity y:

$$\langle n\rangle^{\Omega}_{\text{pA}} \cdot \sigma^{tot}_{\text{pA}} = A \int_{\Omega} \frac{dk^*_z}{k^*_0}\, d^2\mathbf{k}_\perp\, f(x,k_\perp) = 2\pi\, A \int_{\Omega} dy\, dk_\perp\, k_\perp\, f(\, x(y,k_\perp),\, k_\perp\,)\,, \tag{19}$$

where

$$y \equiv \frac{1}{2} \ln \frac{k^*_0 + k^*_z}{k^*_0 - k^*_z}\,, \qquad dy = \frac{dk^*_z}{k^*_0}\,, \tag{20}$$

According to (20), for given y and $k_\perp$, the values of k^*_z and k^*_0 are provided by the formulas

$$k^*_z = \mu_\perp \sinh y\,, \qquad k^*_0 = \mu_\perp \cosh y\,, \qquad \mu_\perp \equiv \sqrt{k^2_\perp + \mu^2}\,. \tag{21}$$

Then, we can calculate $x(y,k_\perp)$ by solving the Equation (2) with (3) and (4). For pions, we find the following:

$$x = \frac{k^*_z p^* + k^*_0 E^* - \mu^2/2}{k^*_z p^* - k^*_0 E^* + s/2 - 2m^2} \tag{22}$$

and for protons

$$x = \frac{k^*_z p^* + k^*_0 E^* - m^2}{k^*_z p^* - k^*_0 E^* + s/2 - m^2}\,. \tag{23}$$

Here, E^* and p^* are the energy and momentum, respectively, of the incident proton in the center-of-mass system of NN collisions:

$$E^* = \sqrt{s}/2\,, \qquad p^* = \sqrt{s - 4m^2}/2\,, \qquad s \equiv s_{NN}\,. \tag{24}$$

In our calculations, we first performed integration over the transverse momentum $k_\perp$, and then over the rapidity y:

$$\langle n\rangle_{\text{pA}} \cdot \sigma^{tot}_{\text{pA}} = 2\pi\, A \int_{-1}^{-0.5} dy \int_{k^{min}_\perp(y)}^{k^{max}_\perp(y)} dk_\perp\, k_\perp\, f(\, x(y,k_\perp),\, k_\perp\,)\,. \tag{25}$$

The limits of integration over the transverse momentum $k_\perp$ were specified by setting the minimum and maximum values of the cumulative number under consideration:

$$k^{min}_\perp(y) = k_\perp(y, x_{min}) \qquad k^{max}_\perp(y) = k_\perp(y, x_{max}) \tag{26}$$

where $k_\perp(y,x)$ is defined by the formulas

$$k_\perp(y,x) = \sqrt{\mu^2_\perp(y,x) - \mu^2}\,, \qquad \mu_\perp(y,x) = \frac{\bar{s}(x)/2}{E^*(x+1)\cosh y + p^*(x-1)\sinh y}\,. \tag{27}$$

The value of $\bar{s}(x)$ is provided by (3) and (4) for pions and protons, respectively.

These limits of integration over transverse momentum $k_\perp$ are of practical interest, as they determine the interval of transverse momenta $k_\perp$ for a given rapidity y, in which particles with given values of the cumulative number must be registered in the experiment.

The difficulty of experimentally measuring the predicted effects lies in the fact that a given interval of change in the cumulative number x at a fixed value of the particle's rapidity corresponds to a certain interval of its transverse momenta, which depends on both the initial energy and the type of particle being detected (see the yellow region C in Figures 1 and 2). In the general case, the boundaries of the transverse momentum interval in which particles with given values of the cumulative number should be detected in the experiment are easily calculated using Formulas (26) and (27).

In Table 1, we present them for the production of cumulative pions and protons for two values of the cumulative number x = 1.6 and 3.0 and values of rapidity $y = -1$ and -0.5 for two initial energies $\sqrt{s_{NN}} = 4$ and 8 GeV. From this table, it can be seen that the transverse momenta at an initial energy of 8 GeV are approximately two times greater than at 4 GeV (see Figures 1 and 2).

Table 1. Minimum ($k_{\perp}^{min}$) and maximum ($k_{\perp}^{max}$) transverse momenta of cumulative pions and protons corresponding to the values of the cumulative number x = 1.6 and 3.0 for given values of rapidity y and initial energy.

$\sqrt{s_{NN}}$	**4 GeV**			**8 GeV**		
	y	$k_{\perp}^{min}$	$k_{\perp}^{max}$	y	$k_{\perp}^{min}$	$k_{\perp}^{max}$
π	−1.	1.468	2.282	−1.	3.634	5.833
	−0.5	1.876	2.605	−0.5	4.602	6.484
p	−1.	1.549	2.547	−1.	3.691	5.988
	−0.5	2.112	2.952	−0.5	4.728	6.671

The results of our calculations of pion and proton multiplicities using the Formula (25) in the new cumulative region at $x \in (1.6, 3.0)$ and $y \in (-1, -0.5)$ (region C in Figures 1 and 2) for pAu collisions are presented in Table 2. For the dependence of particle yields in the cumulative region on transverse momentum, we used dependencies (11) and (14), obtained within the framework of the theoretical approach [16–21] presented in the previous section.

For comparison, we carried out similar calculations using the Gaussian dependence on the transverse momentum (7), as used in the original experimental works [9,10], and with the exponential dependence (7) proposed in [31,32]. The value $x = 1.6$ was chosen as the beginning of the cumulative region because the fits used in these works are valid for both pions and protons when starting from this value. For the total cross section of the pAu interaction, we used the value $\sigma_{\mathrm{pAu}}^{tot}$ = 2 barns.

From Table 2 it can be seen that, at an initial energy of 4 GeV, the predictions for particle multiplicities obtained within the framework of the described theoretical model are consistent to within approximately an order of magnitude with the results obtained using both Gaussian and exponential fits of the experimental data. At an initial energy of 8 GeV, the results of the present theoretical calculations support the results obtained using the more natural exponential fits for the transverse momentum dependence proposed in [31,32], while the use of Gaussian type fits [9,10] predicts extremely low particle multiplicities into this new cumulative region at this energy.

The reason for this is, of course, that at an initial energy of 8 GeV the transverse momenta in the new cumulative region C (see Figures 1 and 2 and Table 1) are approximately two times greater than at 4 GeV.

Table 2. Pion and proton integrated multiplicities in the new cumulative region at $x \in (1.6, 3.0)$ and $y \in (-1, -0.5)$ (region C in Figures 1 and 2) for pAu collisions calculated with the transverse momentum dependences (11) and (14) obtained in the theoretical approach [16–21] (Theor) for initial energies of 4 and 8 GeV, and the same with the Gaussian dependence (7) used in the experimental works [9,10] (Gauss) and the exponential dependence (7) proposed in [31,32] (Exponent).

$\sqrt{s_{NN}}$	4 GeV			8 GeV		
$k_\perp$ **Fit Type**	**Gauss**	**Exponent**	**Theor.**	**Gauss**	**Exponent**	**Theor.**
$\langle n_\pi \rangle_{\text{pAu}}$	$3{\cdot}10^{-6}$	$9{\cdot}10^{-6}$	$1.1{\cdot}10^{-5}$	$1.4{\cdot}10^{-13}$	$7{\cdot}10^{-7}$	$1.9{\cdot}10^{-6}$
$\langle n_{\text{p}} \rangle_{\text{pAu}}$	$2.4{\cdot}10^{-6}$	$1.5{\cdot}10^{-4}$	$7{\cdot}10^{-5}$	$2{\cdot}10^{-24}$	$1.4{\cdot}10^{-8}$	$5{\cdot}10^{-8}$

5. Estimates of Cumulative Production in the Region Available for Study with NICA MPD

Using the estimates of the cumulative production in pAu collisions in the rapidity region $-1 < y < -0.5$ (region C in Figures 1 and 2) made in the previous section, we now try to make a rough estimate of the production of cumulative pions and protons for the symmetric AuAu reaction in the region $0.5 < |y| < 1$ that is available for study with NICA MPD.

Recall that we have excluded the region near zero rapidity, as the theoretical approach [16–21] (Figure 3) used in the present work to describe the transverse momentum dependence of cumulative production (see Section 3) is not valid at small k_z^* values. Another reason for excluding this region from the present consideration is the fact that in this region it may be important to take into account the contribution of the rarer flucton–flucton scattering process [30,33,34]. This process, which is of great physical interest, requires a separate special study, which we leave for our future studies. We only note that such a process can be studied experimentally only in the new cumulative region of central rapidities and large transverse momenta that is available for research using the MPD and SPD facilities of the NICA collider [26–29], and cannot be studied in the traditional cumulative region of fragmentation of one of the nuclei.

In order to obtain estimates for cumulative particles in the $-1 < y < -0.5$ region in the AuAu reaction based on estimates of their yields in this region in the pAu collision, it is necessary to take into account the increased effective flux of nucleons compared to protons, as they will interact with the flucton in the gold nucleus. Of course, it is necessary to take into account that in this case there is a symmetrical contribution to the rapidity region $0.5 < y < 1$, which comes from the interaction of the nucleons of the second nucleus with the flucton of the first nucleus.

Replacing an incident proton with a nucleus increases the number of projectile nucleons interacting with a flucton in another nucleus. To take this into account, we introduce an effective factor γ. The magnitude of this factor can be estimated through the ratio of the number of participating nucleons $\gamma_{part} = \langle N_{part} \rangle_{\text{AuAu}} / \langle N_{part} \rangle_{\text{pAu}}$ or NN collisions $\gamma_{coll} = \langle N_{coll} \rangle_{\text{AuAu}} / \langle N_{coll} \rangle_{\text{pAu}}$ in pAu and AuAu reactions. Clearly, the result will strongly depend on the centrality of the AuAu collision.

At high energies, the values of γ_{part} and γ_{coll} are significantly different. From the ALICE experiment [35–37] we know that, for pPb and PbPb collisions at LHC energies, γ_{part} = 15 for min. bias events and increases to a value of 24 for 0–5% of the most central events, while γ_{coll} = 55 for min. bias events, increasing to 115 for central ones. As is known, the number of participating nucleons N_{part} is determined mainly by the collision geometry (the value of the impact parameter), and weakly depends on the initial energy, while the number of nucleon–nucleon collisions N_{coll} increases significantly with increasing initial energy. Therefore, taking into account the relatively low energies of the NICA collider, for further rough estimates we chose a value of γ equal to γ_{part} = 15 for the case of min. bias collisions.

The obtained estimates of integral multiplicities and yields of pions and protons in min. bias AuAu collisions at the NICA collider in the cumulative region $x \in (1.6, 3.0)$ and

$0.5 < |y| < 1$ due to the process of interaction of a nucleon of one nucleus with a flucton of another are presented in Table 3. The contribution of nucleon–flucton interactions was calculated using the dependences on the transverse momentum (11) and (14) obtained in the theoretical approach [16–21] (see Section 3).

Table 3. Estimates of integral multiplicities and yields of pions and protons in min. bias AuAu collisions in the new cumulative region $x \in (1.6, 3.0)$ and $0.5 < |y| < 1$ available for study with the NICA MPD. The contribution of nucleon–flucton interactions was calculated using the dependences on the transverse momentum (11) and (14) obtained in the theoretical approach [16–21] (see Section 3).

$\sqrt{s_{NN}}$	4 GeV	8 GeV
$\langle n_\pi \rangle_{\text{AuAu}}$	$3{\cdot}10^{-4}$	$6{\cdot}10^{-5}$
$\langle n_\text{p} \rangle_{\text{AuAu}}$	$2{\cdot}10^{-3}$	$1.5{\cdot}10^{-6}$
Y^{π}_{AuAu}	80	1500
$Y^{\text{p}}_{\text{AuAu}}$	500	40

The estimates of cumulative particle yields

$$Y_{\text{AuAu}} = \langle n \rangle_{\text{AuAu}} \cdot R_{\text{AuAu}} \cdot t \tag{28}$$

in Table 3 are presented for one hour (t) of operation of the NICA collider. When performing them, we took into account that the design luminosity of the NICA collider for AuAu collisions at an energy of 8 GeV will be 100 times higher than at an energy of 4 GeV ($L_{\text{AuAu}} = 10^{27}$ and 10^{25} cm^{-2}s^{-1}, respectively), resulting in interaction rates

$$R_{\text{AuAu}} = L_{\text{AuAu}} \cdot \sigma^{tot}_{\text{AuAu}} \tag{29}$$

of 7 kHz and 70 Hz with $\sigma^{tot}_{\text{AuAu}} \approx 7$ barns, which corresponds to the values in [26].

When analyzing the yields of cumulative particles presented in Table 3, it is necessary to keep in mind that they refer to the case of an “ideal” detector, and provide only an upper limit on the number of detected particles. Despite the fairly high overall efficiency of detecting charged particles at the NICA MPD (about 80–90% [28]), in a real experiment the final number of “good” events that have been selected according to various criteria, such as the position of the interaction vertex, the activation of various triggers, etc., usually turns out to be significantly less (about an order of magnitude) than that provided by general estimates.

From the Y_{AuAu} values in Table 3, it is apparent that the increase in the NICA collider luminosity with increasing initial energy from 4 to 8 GeV practically compensates for the overall drop of the integral multiplicities $\langle n \rangle_{\text{AuAu}}$ arising due to the general increase of transverse momenta in the cumulative region with energy. This allows us to conclude that it is possible to observe the production of particles in the new cumulative region of central rapidities and high transverse momenta in Au–Au collisions using the MPD installation of the NICA complex at initial energies of both 4 and 8 GeV.

Conducting research at higher energies of the NICA collider, for example, at $\sqrt{s_{NN}}$ = 11 GeV, is more difficult, as a further drop in integral multiplicities $\langle n \rangle_{\text{AuAu}}$ will no longer be compensated by an increase in luminosity, which remains at the same level at 11 GeV as at 8 GeV [26–28].

To study the dependence of the production of pions and protons on the cumulative number within the described theoretical approach, we calculated the inclusive cross-section

$$\frac{d\sigma}{dx} = \frac{\langle n \rangle^{\Delta x}_{\text{AuAu}}}{\Delta x} \sigma^{tot}_{\text{AuAu}} \tag{30}$$

characterizing the distribution of cumulative particles in x. The results of the calculations are presented in the Figure 5. Note that the errors presented in the figure reflect only the uncertainties arising within the framework of the model.

From Table 3 and Figure 5, it can be seen that when the energy increases, the proton yield decreases much faster than the pion yield for the same fixed value of the cumulative number x. At 4 GeV, the ratio of proton yields to pion yields is about 10 for the same value of x, while at 8 GeV the pion yield already dominates the proton yield more than ten-fold. Recall that in the traditional cumulative region of nucleus fragmentation at low values of transverse momenta, the ratio of proton and pion yields is about 10^4 for the same value of x (see the values of the constants $C_{0\text{p}}$ and $C_{0\pi}$ in the paragraph after Formula (6)).

This effect occurs due to different mechanisms of particle formation with momentum outside the pp-kinematics, that is, coherent coalescence (recombination) of three flucton quarks for a proton and fragmentation of one flucton quark for a pion, in the theoretical approach [16–21] described in Section 3.

There have been some experimental indications that such an effect does occur. Results of the SPIN collaboration on the production of protons and pions with large transverse momenta at an angle of 40° on stationary nuclear targets by protons with an energy of 50 GeV/c ($\sqrt{s_{NN}}$ = 9.8), which corresponds to the cumulative number x up to 1.2, show [38] that in this region the ratio p/π for the same value of the cumulative number x is on the order of 100, which is significantly less than 10^4 in the traditional cumulative region of nucleus fragmentation.

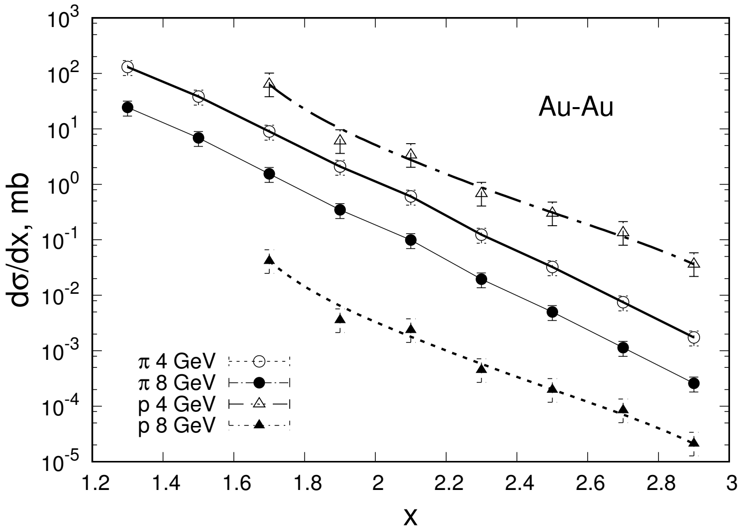

Figure 5. Inclusive cross-sections for the production of pions (○,●) and protons (△,▲) in Au–Au collisions, integrated over rapidity intervals $0.5 < |y| < 1$ and available for study using NICA MPD, as a function of the respective cumulative number x for initial energies of $\sqrt{s_{NN}}$ = 4 and 8 GeV (the lines serve as a visual guide).

It is assumed that the obtained dependences will be studied in MPD and SPD experiments at the NICA collider [26–29] using existing and new ultra-thin pixel detector systems. It is important to note that for reliable registration of very rare events of particle creation in the cumulative region and reliable separation of their tracks from various kinds of false background tracks, it is necessary to simultaneously obtain a signal from several different types of detectors used by the MPD installation [28]. In this regard, information from the internal tracking system [39] is especially important, making it possible to reliably confirm the exit of the track of a cumulative particle from the vertex of the primary interaction and thereby isolate it from the inevitable background noise.

6. Conclusions

A consequence of the presence of nuclear density fluctuations in colliding nuclei (so-called fluctons [3]) is the production of particles with momentum in the region outside the nucleon–nucleon kinematics, called cumulative [4]. From the contemporary point of view, these multi-nucleon fluctons that occasionally appear in nuclei are clumps of dense cold baryon-enriched quark–gluon matter. Therefore, studying the process of nucleon scattering on such nuclear density fluctuations with the production of a particle in the cumulative region is of great interest.

In this work, we estimate the yields of pions and protons caused by the interaction of one of the nucleons of a nucleus with a flucton in another nucleus within the new cumulative region of central rapidities and large transverse momenta now available for study at the MPD and SPD facilities of the NICA collider [26–29].

Calculations were carried out using a previously developed microscopic approach [16–21], allowing us to describe the dependence of particle yields on transverse momentum at different values of the cumulative number simultaneously for both pions and protons using a single parameter, namely, the mass of the constituent quark m_q = 310 MeV.

It is shown that the values of pion and proton yields found in this new cumulative region indicate the possibility of studying this phenomenon in collisions of heavy nuclei at the MPD facility of the NICA complex at low initial energies of 4–8 GeV.

Theoretical calculations predict that in this region of initial energies, the dominance of proton yields over pions is replaced by dominance of pion yields when changing from 4 to 8 GeV. This effect arises due to different mechanisms of particle formation in the interaction of a nucleon with a flucton within the framework of the theoretical approach [16–21] (fragmentation of one flucton quark for pion production and coherent fusion (recombination) of three flucton quarks for proton production; see Section 3).

However, when drawing these conclusions it is necessary to keep in mind that in this work only the contribution of the interaction of a nucleon with a flucton was taken into account; the rarer process of flucton–flucton scattering [30,33,34], which was not taken into account, can have a significant contribution, especially in the region of the most central rapidities $|y| < 0.5$. The process of flucton interaction is of great physical interest, and requires a separate special study, which we leave for our future research. It is important that this process can be studied experimentally only in the new cumulative region of central rapidities and large transverse momenta available for research at the MPD and SPD facilities of the NICA collider, and cannot be studied in the traditional cumulative region of fragmentation of one of the nuclei.

7. Summary

The production of particles outside the region allowed by the kinematics of nucleon–nucleon collisions is calculated due to interactions involving dense cold clusters of quark–gluon matter in nuclei. Calculations were carried out using a previously developed microscopic approach [16–21], making it possible to describe dependence of particle yields on transverse momentum at different values of the cumulative number simultaneously for both pions and protons using a value of 310 MeV for a single parameter, namely, the mass of the constituent quark.

Based on these calculations, the possibility of observing this process in the region of central rapidities and large transverse momenta in collisions of heavy ions at low energies at the MPD facility of the NICA collider complex has been demonstrated.

The theoretical calculations predict an increasing dominance of pion yields over protons in this region as the initial energy of nuclear collisions increases from 4 to 8 GeV, which is due to their different mechanisms of formation.

Author Contributions: Conceptualization, V.V.; methodology, V.V.; software, S.B. and S.Y.; validation, V.V.; formal analysis, V.V.; investigation, V.V., S.B. and S.Y.; data curation, S.B. and S.Y.; writing—

original draft preparation, V.V.; writing—review and editing, V.V. and S.Y.; visualization, S.B. and S.Y.; supervision, V.V. All authors have read and agreed to the published version of the manuscript.

Funding: This research was funded by the Russian Science Foundation, grant number 23-12-00042.

Data Availability Statement: Data are contained within the article.

Acknowledgments: The authors are grateful to Grigory Feofilov for stimulating discussions.

Conflicts of Interest: The authors declare no conflicts of interest.

Abbreviations

The following abbreviations are used in this manuscript:

NICA	Nuclotron-based Ion Collider fAcility
MPD	Multi-Purpose Detector
SPD	Spin Physics Detector
JINR	Joint Institute for Nuclear Research
FAIR	Facility for Antiproton and Ion Research
ALICE	A Large Ion Collider Experiment
LHC	Large Hadron Collider
RHIC	Relativistic Heavy Ion Collider

References

1. Leksin, G.A. Elastic and Quasi-Elastic Scattering of 660 MeV Protons by Deuterons. *Sov. Phys. JETP* **1957**, *5*, 371–377.
2. Azhgirei, L.S.; Vzorov, I.K.; Zrelov, V.P.; Meshcheriakov, M.G.; Neganov, B.S.; Shabudin, A.F. Knockout of Deuterons from Li, Be, C, and O Nuclei by Protons of Energy 675 MeV. *Sov. Phys. JETP* **1958**, *6*, 911–919.
3. Blokhintsev, D.I. On the Fluctuations of Nuclear Matter. *Sov. Phys. JETP* **1958**, *6*, 995–999.
4. Baldin, A.M.; Gerasimov, S.B.; Guiordenescu, H.; Zubarev, V.N.; Ivanova, L.K.; Kirillov, A.D.; Kuznetsov, V.A.; Moroz, N.S.; Radomanov, V.B.; Ramzhin, V.N.; et al. Cumulative meson production. *Sov. J. Nucl. Phys.* **1974**, *18*, 41–44.
5. Papp, J.; Jaros, J.; Schroeder, L.; Staples, J.; Steiner, H.; Wagner, A.; Wiss, J. Inclusive Pion Production in Collisions of Relativistic Protons, Deuterons, Alphas, and Carbon Ions with Nuclei. *Phys. Rev. Lett.* **1975**, *34*, 601–604. [CrossRef]
6. Baldin, A.M.; Bondarev, V.K.; Giordenescu, N.; Golovanov, L.B.; Mazarsky, V.L.; Manyatovsky, A.N.; Moroz, N.S.; Panebrattsev, Y.A.; Pentsya, M.; Povtoreiko, A.A.; et al. *Experimental Data on Cumulative Pion Production at 8.9-GeV/c Proton Interaction with Light Nuclei*; Preprint JINR-1-82-28; Joint Institute for Nuclear Research (JINR): Dubna, Russia, 1982.
7. Ableev, V.G.; Abdushukurov, D.A.; Avramenko, S.A.; Dimitrov, C.; Filipkowski, A.; Kobushkin, A.P.; Nikitin, D.K.; Nomofilov, A.A.; Piskunov, N.M.; Sharov, V.I.; et al. A study of the proton momentum spectrum from deuteron fragmentation at 8.9 GeV/c and an estimate of admixture parameters for the six-quark state in the deuteron. *Nucl. Phys. A* **1983**, *393*, 491–501. [CrossRef]
8. Boyarinov, S.V.; Evseev, I.I.; Kiselev, Y.T.; Leksin, G.A.; Martemyanov, A.N.; Mikhailov, K.R.; Pozdnyakov, S.A.; Polozov, P.A.; Sheinkman, V.A.; Terekhov, Y.V.; et al. The Properties of nuclear matter at small distances. *Sov. J. Nucl. Phys.* **1992**, *55*, 917–921.
9. Boyarinov, S.V.; Gerzon, S.A.; Kats, M.M.; Kiselev, Y.T.; Leksin, G.A.; Martemyanov, A.N.; Novikov, V.L.; Semenov, S.V.; Terekhov, Y.V.; Sheinkman, V.A. Production of Cumulative Protons at Momenta 0.6 GeV/c to 1.83 GeV/c. *Sov. J. Nucl. Phys.* **1987**, *46*, 871–876.
10. Boyarinov, S.V.; Evseev, I.I.; Kiselev, Y.T.; Leksin, G.A.; Martemyanov, A.N.; Mikhailov, K.R.; Pozdnyakov, S.A.; Terekhov, Y.V.; Ushakov, V.I.; Sheinkman, V.A. Yields of p, anti-p, pi+-, and K+- emitted at an angle of 97 degrees in the laboratory system from nuclei irradiated by 10.14 GeV protons. *Phys. Atom. Nucl.* **1994**, *57*, 1379–1388.
11. Efremov, A.V. Quark-parton picture of the cumulative production. *Prog. Part. Nucl. Phys.* **1982**, *8*, 345–365. [CrossRef]
12. Burov, V.V.; Lukyanov, V.K.; Titov, A.I. Large momentum pion production in proton nucleus collisions and the idea of fluctuons in nuclei. *Phys. Lett. B* **1977**, *67*, 46–48. [CrossRef]
13. Schmidt, I.A.; Blankenbecler, R. Relativistic interactions between nuclei. *Phys. Rev. D* **1977**, *15*, 3321. [CrossRef]
14. Frankfurt, L.L.; Strikmann, M.I. High-energy phenomena, short-range nuclear structure and QCD. *Phys. Rep.* **1981**, *76*, 215–347. [CrossRef]
15. Efremov, A.V.; Kaidalov, A.B.; Kim, V.T.; Lykasov, G.L.; Slavin, N.V. Production of cumulative hadrons in quark models of flucton fragmentation. *Sov. J. Nucl. Phys.* **1988**, *47*, 868–874.
16. Braun, M.A.; Vechernin, V.V. Nuclear Structure Functions and Particle Production in the Cumulative Region in the Parton Model. *Nucl. Phys. B* **1994**, *427*, 614–640. [CrossRef]
17. Braun, M.A.; Vechernin, V.V. Structure Functions and Particle Production in the Cumulative Region: Two different exponentials. *Phys. At. Nucl.* **1997**, *60*, 432–438.
18. Braun, M.A.; Vechernin, V.V. Transverse-momentum dependence of cumulative pions. *Phys. At. Nucl.* **2000**, *63*, 1831–1834. [CrossRef]

19. Braun, M.A.; Vechernin, V.V. Production of cumulative hadrons in quark models of flucton fragmentation. *Nucl. Phys. B—Proc. Suppl.* **2001**, *92*, 156–161. [CrossRef]
20. Braun, M.A.; Vechernin, V.V. Quark coalescence mechanism near the threshold. *Theor. Math. Phys.* **2004**, *139*, 766–786. [CrossRef]
21. Vechernin, V. Transverse momentum dependence of spectra of cumulative particles produced from droplets of dense nuclear matter. *AIP Conf. Proc.* **2016**, *1707*, 060020.
22. Gorenstein, M.I.; Zinovjev, G.M. Cluster model of cumulative particle production in hadron-nucleus collisions. *Phys. Lett. B* **1977**, *67*, 100–102. [CrossRef]
23. Bogatskaya, I.G.; Chiu, C.B.; Gorenstein, M.I.; Zinovjev, G.M. Fireball model for baryonic inclusive spectra in particle-nucleus and nuclei-nucleus collisions at high energy. *Phys. Rev. C* **1980**, *22*, 209–220. [CrossRef]
24. Anchishkin, D.V.; Gorenstein, M.I.; Zinovjev, G.M. Cumulative effect and the model of nuclear fireballs. *Phys. Lett. B* **1982**, *108*, 47–50. [CrossRef]
25. Motornenko, A.; Gorenstein, M.I. Cumulative production of pions by heavy baryonic resonances in proton-nucleus collisions. *J. Phys. G* **2017**, *44*, 025105. [CrossRef]
26. Kekelidze, V.; Kovalenko, A.; Lednicky, R.; Matveev, V.; Meshkov, I.; Sorin, A.; Trubnikov, G. Feasibility study of heavy-ion collision physics at NICA JINR. *Nucl. Phys. A* **2017**, *967*, 884–887. [CrossRef]
27. Kekelidze, V.; Matveev, V.; Meshkov, I.; Sorin, A.; Trubnikov, G. Project Nuclotron-based Ion Collider Facility at JINR. *Phys. Part. Nucl.* **2017**, *48*, 727–741. [CrossRef]
28. Abgaryan, V.; Acevedo Kado, R.; Afanasyev, S.V.; Agakishiev, G.N.; Alpatov, E.; Altsybeev, G.; Hernández, M.A.; Andreeva, S.V.; Andreeva, T.V.; Andronov, E.V.; et al. Status and initial physics performance studies of the MPD experiment at NICA. *Eur. Phys. J. A* **2022**, *58*, 140. [CrossRef]
29. Abazov, V.M.; Abramov, V.; Afanasyev, L.G.; Akhunzyanov, R.R.; Akindinov, A.V.; Akopov, N.; Alekseev, I.G.; Aleshko, A.M.; Alexakhin, V.Y.; Alexeev, G.D.; et al. Conceptual design of the Spin Physics Detector. *arXiv* **2022**, arXiv:2102.00442v3.
30. Denisovskaya, O.; Mikhailov, K.; Polozov, P.; Prokudin, M.; Sharkov, G.; Stavinsky, A.; Stolin, V.; Tolochek, R.; Tolstoukhov, S. Dense Cold Nuclear Matter Study with Cumulative Trigger. Proposal. *arXiv* **2009**, arXiv:0911.1658.
31. Vechernin, V.V. Yield of particles in the cumulative region at central rapidities and large transverse momenta at the NICA collider. *Phys. Part. Nucl.* **2022**, *53*, 433–440. [CrossRef]
32. Vechernin, V.V. Clusters of cold dense nuclear matter and their registration with the MPD vertex detector. *Phys. Part. Nucl.* **2021**, *52*, 604–608. [CrossRef]
33. Alekseev, I.G.; Vishnyakov, V.E.; Golutvin, A.I.; Goryachev, V.S.; Dzubenko, G.B.; Dolgolenko, A.G.; Zagreev, B.V.; Kiselev, S.M.; Korolko, I.E.; Leksin, G.A.; et al. Measurement of cumulative-photon spectra at high transverse momenta in $^{12}C^{9}Be$ interactions at an energy of 3.2 GeV per nucleon. *Phys. Atom. Nucl.* **2008**, *71*, 1848–1859. [CrossRef]
34. Stavinskiy, A. Dense Cold Matter with Cumulative Trigger. *Phys. Part. Nucl. Lett.* **2011**, *8*, 912–914. [CrossRef]
35. Abelev, B.; Adam, J.; Adamová, D.; Adare, A.M.; Aggarwal, M.M.; Rinella, G.A.; Agnello, M.; Agocs, A.G.; Agostinelli, A.; Ahammed, Z.; et al. Centrality determination of Pb-Pb collisions at 2.76 TeV with ALICE. *Phys. Rev. C* **2013**, *88*, 044909. [CrossRef]
36. Adam, J.; Adamová, D.; Aggarwal, M.M.; Rinella, G.A.; Agnello, M.; Agostinelli, A.; Agrawal, N.; Ahammed, Z.; Ahmed, I.; Ahn, S.U.; et al. Centrality dependence of particle production in p-Pb collisions at 5.02 TeV. *Phys. Rev. C* **2015**, *91*, 064905. [CrossRef]
37. Loizides, C.; Kamin, J.; d'Enterria, D. Improved Monte Carlo Glauber predictions at present and future nuclear colliders. *Phys. Rev. C* **2019**, *99*, 019901. [CrossRef]
38. Semak, A. High pt anti-proton and meson production in cumulative pA reaction at 50 GeV/c. In Proceedings of the LXX International Conference "NUCLEUS–2020. Nuclear Physics and Elementary Particle Physics. Nuclear Physics Technologie", St. Petersburg, Russia, 11–17 October 2020. Available online: https://indico.cern.ch/event/839985/contributions/3983657/attachments/2124000/3576745/NUCLEUS_2020_Semak.pdf (accessed on 17 October 2020).
39. Zherebchevsky, V.I.; Kondratiev, V.P.; Vechernin, V.V.; Igolkin, S.N. The concept of the MPD vertex detector for the detection of rare events in Au+Au collisions at the NICA collider. *Nucl. Instrum. Methods Phys. Res. A* **2021**, *985*, 164668. [CrossRef]